The Production of O(^{1}D) in Comet Hale-Bopp

J. P. Morgenthaler, W. Harris, F. Scherb, C. M. Anderson, N. E. Doane, F. L. Roesler,

(University of Wisconsin),

R. J. Oliversen (GSFC), M. R. Combi (University of Michigan)

Received _____; accepted _____

Abstract

Photometric observations of comet Hale-Bopp (C/1995 OI) in the forbidden red line of neutral oxygen ([O I] 6300 Å) with three independent telescopes on Kitt Peak in March of 1997 imply a production rate of the metastable O(^{1}D) of 300–400$\times 10^{28}$ s^{-1}. Using water production rates, Q(H_2O), determined by H_2O, OH, and H measurements (e.g. Dello Russo et al. 2000; Biver et al. 1997; Colom et al. 1997; Combi et al. 2000) and the standard water and OH photodissociation branching ratios found in Huebner et al. (1992) and Van Dishoeck & Dalgarno (1984), we expect 88×10^{28} s^{-1}. Assuming the Q(H_2O) values found elsewhere in the literature are correct, we explore several hypotheses that would account for this excess O(^{1}D) emission, finding that either the OH $\rightarrow$ O(^{1}D) branching ratio of Nee & Lee (1984) should be used in preference to that of Van Dishoeck & Dalgarno or some mechanism other than photodissociation of H_2O and OH, such as electron collisional excitation of neutral oxygen, is producing the bulk of the O(^{1}D) in Hale-Bopp.

Introduction

The release of water from the nucleus and its subsequent photochemical behavior drive much of the physical phenomena in cometary comae when comets approach within $\sim$2 AU of the Sun. Thus, one of the first tasks in understanding any cometary system is to determine that comet's water production rate, Q(H_2O).

Direct emission from water has been detected (e.g. Mumma et al. 1996; Dello Russo et al. 2000), but traditionally, the more easily observed emissions from its daughter products (OH, H, and O) have been the primary means for determining Q(H_2O). We have observed [O I] 6300 Å emission from O(^{1}D) in comets 1973 XII Kohoutek (Huppler et al. 1975; Scherb 1981), 1986 P/Halley (Magee-Sauer et al. 1988; Magee-Sauer et al. 1990; Smyth et al. 1993), 1989c1 Austin (Schultz et al. 1992, 1993), Hyakutake (in preparation),

and C/1995 O1 Hale-Bopp (this work) using Fabry-Perot interferometers with resolving powers high enough to separate the [O I] 6300 Å line from the Earth's airglow line and nearby cometary NH_2 lines (e.g. Figure 3). The wide field of view (FOV) and good sensitivity of our instruments (up to 1° and <1 R) allow for direct detection of almost all the [O I] 6300 Å in a comet, thus minimizing the systematic effects from aperture correction calculations. Furthermore, because [O I] 6300 Å emission is prompt rather than fluorescent, if all these photons come from O(^{1}D) created during the photodissociation of H_2O and its daughter OH, Q(H_2O) can be derived from our wide aperture photometry algebraically (Equation 1) without appeal to models of the temperature, density, outflow velocity, or fluorescent efficiencies (g-factors) of material in the coma. The only quantities in Equation 1 not well determined by our measurements are the branching ratios of the photodissociation reactions.

$$\mathrm{Q}(\mathrm{H_2O}) = \frac{\mathbf{Q}(\mathrm{O}(^1\mathrm{D}))}{BR1 + (BR2)(BR3)} \tag{1}$$

where the branching ratios found in the literature are listed in Table 1 and $\mathbf{Q}(O(^1D))$, the observed O(^{1}D) production rate is given by:

$$\mathbf{Q}(\mathrm{O}(^1\mathrm{D})) = \left(\frac{4}{3}\right)(4\pi\Delta^2\Omega I_{6300})AC. \tag{2}$$

The factor of 4/3 corrects for the emission in the 6364 Å decay path of O(^{1}D), Δ is the distance between the earth and the comet, Ω is the instrument field of view and AC is the aperture correction.

Table 1. Photodissociation Branching Ratios

Reaction	BRn	Ref.[a]	Quiet Sun	Active Sun
$H_2O + h\nu \rightarrow H_2 + O(^1D)$	$BR1$	H	0.050	0.067
$H_2O + h\nu \rightarrow H + OH$	$BR2$	H	0.855	0.801
$OH + h\nu \rightarrow H + O(^1D)$	$BR3$	V	0.048	0.101
$OH + h\nu \rightarrow H + O(^1D)$	$BR3'$	H/N	0.349	0.515
$CO(X^1\Sigma^+) + h\nu \rightarrow C(^1D) + O(^1D)$	$BR4$	H	0.046	0.042
$CO(X^1\Sigma^+) + h\nu \rightarrow C(^1D) + O(^1D)$	$BR4'$	T	0.123	0.123
$CO_2 + h\nu \rightarrow CO(X^1\Sigma^+) + O(^1D)$	$BR5$	H	0.457	0.391

[a]references: H, Huebner et al. (1992); V, Van Dishoeck & Dalgarno (1984); H/N, Huebner et al. (1992) using Nee & Lee (1984) experimental OH cross sections; T Tozzi et al. (1998). The OH cross sections have been calculated for a heliocentric velocity of -14 km/s, appropriate for early March, 1997.

Observations

On 6 nights the Hydra positioner of the 3.5-meter Wisconsin, Indiana, Yale, NRAO (WIYN) Telescope Multi Object Spectrograph (MOS) was used to place up to 96 fibers in concentric rings around the nucleus to as much as 22.5 arc minutes in radius (see Figure 1). The MOS spectra were recorded over a 300 Å range centered at 6250 Å with a resolving power of $(\lambda/\Delta\lambda)$ ~15,000. On 4 nights a 7 by 13 array of 3 arc second fibers on 4 arc second centers known as Densepak was used on the WIYN MOS to probe the inner coma.

On three nights, the 6-inch Fabry-Perot spectrometer that comprises the Wisconsin H-α Mapper (WHAM), recorded narrow band images over a 1° field of view and spectra over a 200 km/s range (4 Å at 6300 Å) with a resolving power of $(\lambda/\Delta\lambda)$ ~30,000.

On 29 nights a 2-inch Fabry-Perot spectrometer on the NSO McMath-Pierce main telescope recorded high resolution ($\lambda/\Delta\lambda$ = 80,000) spectra of

the [O I] 6300 Å emission with a 6 arcminute field of view. The combination of MOS and Fabry-Perot data covers spatial scales ranging from 2,000 km to 1×10^6 km.

We have high confidence in the absolute calibration of the WHAM and WIYN instruments, as they are based on observations of NGC 7000 (the North American Nebula), which has been used as a successful standard candle in decades of work on Galactic and geocoronal H-α emission (e.g. Reynolds 1997; Münch & Pitz 1989; Nossal et al. 1993; Bishop et al. 2000) since Scherb (1981) used standard stars and planetary nebulae to find its surface brightness (850 R in the central 49 arcminutes). The calibration has been confirmed using observations of a well understood black body source (Nossal 1994, chapter 11).

Results

Figure 3 shows all of the [O I] spectra obtained by the WHAM spectrometer together with the curve fit used to find the total surface brightness in the one degree WHAM field of view. Figure 2 shows one of the best spectra from the 2-inch Fabry-Perot instrument. In general, spectral extraction from these data is difficult, as shown by the large scatter in Figure 4 (Doane 1999; Oliversen et al. 2000). High quality [O I] and continuum images of Hale-Bopp were recorded on March 5 and combined to form Figure 1, which was used to calculate AC for the 2-inch FOV. The tailward asymmetry, which contributes ∼13% of the total [O I] emission, is discussed elsewhere (Morgenthaler et al. 1999). Radial profiles from the WHAM image are shown in Figure 6. They compare well to the March 2 Hydra radial profile, which has been calculated excluding the tailward quadrant. We apply equations 1 and 2 to our Fabry-Perot data to arrive at the $Q(H_2O)$ values shown in Table 2 and Figures 4 and 5. The Haser (1957) models shown in Figure 6 were used to calculate the production rates for the MOS data.

Table 2. Comet Hale-Bopp $\mathbf{Q}(O(^1D))$ and $Q(H_2O)$ values[a]

UT date[b]	Inst.[c]	$R_\odot$[d]	$\mathbf{Q}(O(^1D))$[e]	$\mathbf{Q}'(O(^1D))$[f]	$Q(H_2O)$[g]	$Q'(H_2O)$[h]
Feb 22	W	1.129	2.37		26.2	6.82
Feb 24	W	1.110	2.58		28.5	7.43
March 2	H96	1.055	3.21	3.21	35.5	9.24
March 5	W	1.029	3.21		35.5	9.24
March 9	50 mm FP	0.999	3.98		44.0	11.5
March 10	50 mm FP	0.992	3.52		38.9	10.1
March 16	H96	0.956	1.99	2.78	22.0	8.0
March 18	D	0.946	1.99	2.78	22.0	8.0
April 7	50 mm FP	0.920	5.80		64.1	16.7
April 8	50 mm FP	0.923	5.07		56.0	14.6
April 9	50 mm FP	0.925	4.92		54.4	14.2
April 10	50 mm FP	0.928	2.56		28.3	7.4
April 13	50 mm FP	0.939	2.77		30.6	8.0
April 14	50 mm FP	0.943	3.25		35.9	9.3
April 16	50 mm FP	0.952	4.61		50.9	13.3
April 21	H96	0.981	1.36	1.04	15.0	3.0

[a]These $Q(H_2O)$ values are derived assuming photodissociation of H_2O and its daughter OH are the only sources of $O(^1D)$.

[b]1997

[c]W = WHAM, H96 = Hydra, 96 fibers, 50 mm FP = 50 mm Fabry-Perot, D = Densepak

[d]Hale-Bopp heliocentric distance (AU)

[e]$\times 10^{30}$ s^{-1}. Calculated directly with Equation 2 for WHAM and 50 mm Fabry-Perot. For Hydra, calculated using Haser models shown in Figure 6 using Van Dishoeck & Dalgarno (1984) OH excitation rates.

[f]$\times 10^{30}$ s^{-1}. For Hydra, calculated using Haser model using Nee & Lee (1984) OH excitation rates.

[g]$\times 10^{30}$ s^{-1}. WHAM and 50 mm Fabry-Perot results derived with Equation 1 and OH $\rightarrow$ $O(^1D)$ branching ratios based on Van Dishoeck & Dalgarno (1984).

[h]$\times 10^{30}$ s^{-1}. WHAM and 50 mm Fabry-Perot results derived with Equation 1 and OH $\rightarrow$ $O(^1D)$ branching ratios based on Van Dishoeck & Dalgarno (1984).

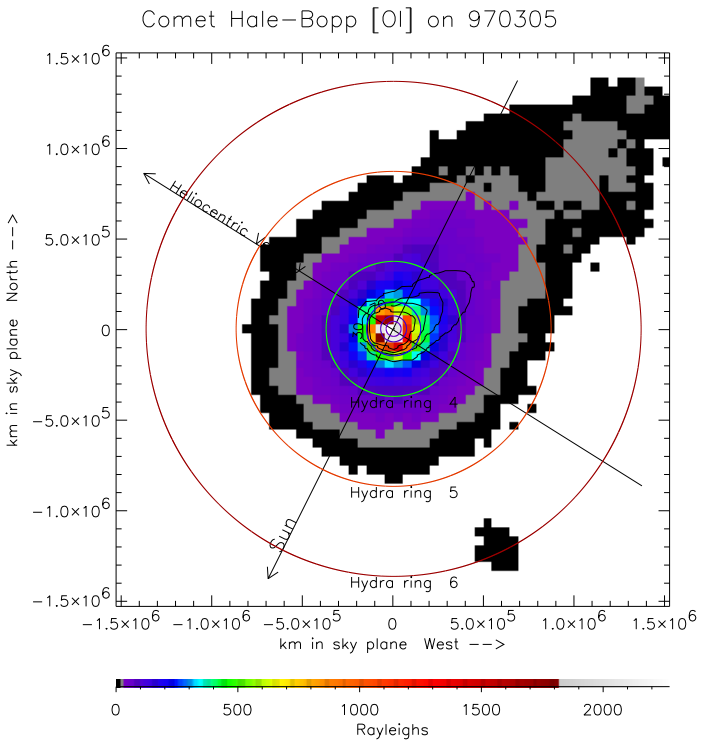

Fig. 1.— Hale-Bopp image with [O I] emission shown in color, dust in contours, and circles showing positions of the Hydra annuli. The WHAM field of view is 1° in diameter.

The Problem

As shown in Figure 4, Q(H_2O) values derived using our [O I] 6300 Å measurements the widely accepted theoretically calculated OH cross sections of Van Dishoeck & Dalgarno (1984) are a factor of 3–4 times higher than the Q(H_2O) values derived by H_2O, OH, and H measurements (e.g. Dello Russo et al. 2000; Biver et al. 1997; Colom et al. 1997; Combi et al. 2000). The quality of our photometry leads to one or more of the following possibilities:

1. Q(H_2O) values derived by all other methods are systematically low
2. Photodissociation of H_2O and OH are not the dominant sources of O(^{1}D) in Hale-Bopp
3. There is a problem with the $H_2O \rightarrow O(^1D)$ branching ratio calculated from excitation rates in Huebner et al. (1992)

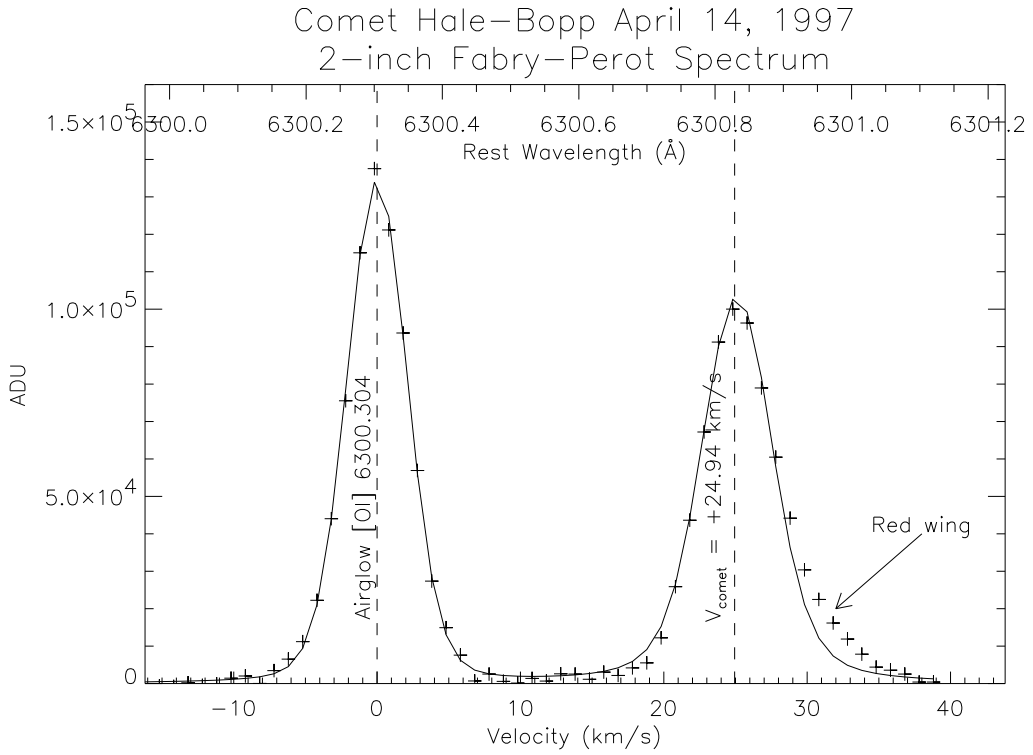

Fig. 2.— One of the better 2 inch Fabry-Perot spectra of comet Hale-Bopp taken on April 14, 1997. The field of view is 200,000 km in radius, centered on the comet head. The red tail on the velocity distribution is consistent with material flowing tail-ward.

4. There is a problem with the OH $\rightarrow$ O(^{1}D) branching ratio calculated from excitation rates in Van Dishoeck & Dalgarno (1984)

Given the agreement in the Q(H_2O) values derived by several techniques, scenario (1) seems unlikely. However, it is important to note that all these methods depend critically on the photodissociation lifetime of H_2O and/or OH. Due to uncertainties in the cross sections and solar UV spectrum, these quantities are probably uncertain to at least the several tens of percent level (e.g. Cochran & Schleicher 1993). A critique of the validity of these lifetimes is beyond the scope of this work and we assume that the other authors have considered these problems, so, we will discount possibility (1).

Other Sources of O(^{1}D)

Since CO and CO_2 are the next most abundant parent species after H_2O in cometary comae, we consider their contribution to the total observed O(^{1}D) flux in comet Hale-Bopp. We calculate an upper limit using the branching ratios listed in Table 1, the CO production rate measured by Biver et al. (1997) and the assumption that *all* CO is a daughter of photodissociating CO_2. As shown in the 5th and 6th columns Table 3, even in this extreme case, the contribution of photodissociation CO and CO_2 to the total O(^{1}D) production is negligible compared to that of H_2O and OH. Using Haser models, ionization cross sections are from Huebner et al. (1992) and dissociative recombination rates from Le Teuff et al. (2000) of H_2O, OH, CO, and CO_2, we find the contributions of dissociative recombination and collisional dissociation are also negligible.

Electron Excitation

Evidence for electron collisions with neutral oxygen is found in [O I] 1356 Å emission detected by McPhate et al. (1999). Simple models based on Haser calculations and the data of McPhate et al. are unable to rule out the possibility that electron collisions contribute significantly to the O(^{1}D) production rate. However, the resulting O(^{1}D) radial profile would have to very closely mimic that of our Haser models (Figure 6).

H_2O and OH Branching Ratios

We find no evidence in the literature that the $H_2O \rightarrow$ O(^{1}D) branching ratio is significantly different than that found in Huebner et al. Furthermore, the branching ratio does not seem to be particularly sensitive to solar activity, so we discount possibility (3).

In support of possibility (4), we find the OH $\rightarrow$ O(^{1}D) branching ratio calculated using the experimental OH cross sections of Nee & Lee (1984) is

Table 3. Estimated Production Rates and Contributions to O(^{1}D) Emission in Hale-Bopp on March 04–06, 1997

Date	Species (x)	Ref.[a]	Q(x)[bc]	Q_x(O(^{1}D))[c]	Q_x(O(^{1}D))[c]
Mar 05	O(^{1}D)	This work	320	320	320
Mar 06	H_2O	C,H	970	48	
Mar 04	OH	B,V/N	610	29[d]	210[e]
Mar 06	OH	$BR2\times$C, V/N	830	40[d]	290[e]
Mar 06	CO	B,H	160	7	
Mar 06	CO	B,T	160	2	
Mar 06	CO_2	B/($BR4 + BR5$),H	340	160	
Mar 06	CO_2	C$\times$W,H	39	18	

[a]References: production rates are reported by C, Combi et al. (2000) and B, Biver et al. (1997). Branching ratios are from H, Huebner et al. (1992); V, Van Dishoeck & Dalgarno (1984); N, Nee & Lee (1984); and T, Tozzi et al. (1998). The ratio H_2O/CO_2 of 4% is from Weaver et al. (1994).

[b]production rate ($\times 10^{28}$ s^{-1})

[c]contribution to the O(^{1}D) production rate ($\times 10^{28}$ s^{-1})

[d]Van Dishoeck & Dalgarno (1984) OH $\rightarrow$ O(^{1}D) branching ratio

[e]Nee & Lee (1984) OH $\rightarrow$ O(^{1}D) branching ratio

a factor of 7 higher than that of Van Dishoeck & Dalgarno (Huebner et al. 1992). Using the Nee & Lee OH $\rightarrow$ O(^{1}D) branching ratio, our Q(O(^{1}D)) values agree with other results (Figure 5). However, using the Nee & Lee OH lifetime in our Haser models, we find an outflow velocity of $\sim 8 \pm 1$ km s^{-1}, which is incompatible with the observed outflow velocity of 2.2 km s^{-1} calculated from OH radio line profiles (Colom et al. 1997). Assuming the outflow velocity measured by Colom et al. and the OH lifetime of Nee & Lee, we cannot match the shape of our [O I] 6300 Å radial profiles, even if the H_2O excitation rates are allowed to vary from their accepted values.

Conclusion

We have recorded [O I]6300 Å data with three different instruments, two Fabry-Perot spectrometers (calibrated against NGC 7000) and a multi-object spectrograph (calibrated against standard stars). All three of these datasets show consistent [O I] production rates. Converting these [O I] rates into Q(H_2O) values using the Huebner et al. (1992) $H_2O \rightarrow$ O(^{1}D) and Van Dishoeck & Dalgarno (1984) OH $\rightarrow$ O(^{1}D) branching ratios results in Q(H_2O) values that are high by a factor of 3-4 when compared with Q(H_2O) values determined by H_2O, OH, and H measurements. We can rule out all possible sources for this discrepancy except for electron excitation or an error in the Van Dishoeck & Dalgarno (1984) OH $\rightarrow$ O(^{1}D) branching ratio. We favor the latter choice, since by using the OH $\rightarrow$ O(^{1}D) branching ratio of Nee & Lee (1984), which is a factor of 7 higher than that of Van Dishoeck & Dalgarno, we achieve good agreement with other Q(H_2O) values. We do not advocate adopting the Nee & Lee OH lifetime, since that implies a bulk OH outflow velocity inconsistent with other measurements.

We would like to thank S. L. Tufte, L. M. Haffner for their help with data acquisition, J. McPhate for providing an electronic copy of Figure 1 of McPhate et al. (1999), and R. Reynolds, F. Roesler, G. Ballester, and W. Smyth for valuable discussions. This work has been supported under NSF grant AST-9615625 and NASA grant NAG 5-7952.

REFERENCES

Bishop, J., Harlander, J., Nossal, S., & Roesler, F. 2000, J. Atmos. Sol.-Terr. Phys., accepted for publication pending revisions

Biver, N., Bockelée–Morvan, D., Colom, P., Crovisier, J., Germain, B., Lellouch, E., Davies, J., Dent, W., Moreno, R., Paubert, G., Wink, J., Despois, D., Lis, D., Mehringer, D., Benford, D., Gardner, M., Phillips, T., Gunnarsson, M., Rickman, H., Winnberg, A., Bergman, P., Johansson, L., & Rauer, H. 1997, Earth, Moon, Planets, 78, 5

Cochran, A. L. & Schleicher, D. G. 1993, Icarus, 105, 235

Colom, P., Gérard, E., Crovisier, J., & Bockelée-Morvan, D. 1997, Earth, Moon, Planets, 78, 37

Combi, M. R., Reinard, A. A., Bertaux, J., Quemerais, E., & Mäkinen, T. 2000, Icarus, 144, 191

Dello Russo, N., DiSanti, M. J., Magee-Sauer, K., Novak, R., & Rettig, T. W. 2000, Icarus, 143, 324

Doane, N. E. 1999, Bachelor's thesis, University of Maryland, journal article in preparation

Haser, L. 1957, Bull. Soc. Roy. Sci. Liège, 43, 740

Huebner, W. F., Keady, J., & Lyon, S. 1992, Astrophys. Space Sci., 195, 1

Huppler, D., Reynolds, R. J., Roesler, F. L., Scherb, F., & Trauger, J. 1975, ApJ, 202, 276

Le Teuff, Y. H., Millar, T. J., & Markwick, A. J. 2000, A&A, in Press

Magee-Sauer, K., Roesler, F. L., Scherb, F., Harlander, J., & Oliversen, R. J. 1988, Icarus, 76, 89

Magee-Sauer, K., Scherb, F., Roesler, F. L., & Harlander, J. 1990, Icarus, 84, 154

McPhate, J. B., Feldman, P. D., McCandliss, S. R., & Burgh, E. B. 1999, ApJ, 521, 920

Morgenthaler, J. P., Scherb, F., Anderson, C. W., Roesler, F. L., Oliversen, R. J., Doane, N. E., Smyth, W. H., & Marconi, M. L. 1999, in American Astronomical Society Meeting, Vol. 194, 1501+

Mumma, M. J., Di Santi, M. A., Dello Russo, N., Fomenkova, M., Magee-Sauer, K., Kaminski, C. D., & Xie, D. X. 1996, Sci, 272, 1310

Münch, G. & Pitz, E. 1989, in The Galactic and Extragalactic Background Radiation (139th IAU Symposium), ed. S. Bowyer & C. Leinert, IAU (Boston: Kluwer), 193–198

Nee, J. B. & Lee, L. C. 1984, J. Chem. Phys., 81, 31

Nossal, S. 1994, PhD thesis, University of Wisconsin–Madison

Nossal, S., Reynolds, R. J., Roesler, F. L., Scherb, F., & Harlander, J. 1993, J. Geophys. Res., 98, 3669

Oliversen, R. J., Doane, N. E., Scherb, F., et al. 2000, In preparation

Reynolds, R. J. 1997, Science, 277, 1446

Scherb, F. 1981, ApJ, 243, 644

Schultz, D., Li, G. S. H., Scherb, F., & Roesler, F. 1993, Icarus, 101, 95

Schultz, D., Li, G. S. H., Scherb, F., & Roesler, F. L. 1992, Icarus, 96, 190

Smyth, W. H., Marconi, M. L., Scherb, F., & Roesler, F. 1993, ApJ, 413, 756

Tozzi, G. P., Feldman, P. D., & Festou, M. C. 1998, A&A, 330, 753

Van Dishoeck, E. F. & Dalgarno, A. 1984, Icarus, 59, 305

Weaver, H. A., Feldman, P. D., & McPhate, J. B. 1994, ApJ, 422, 374

This manuscript was prepared with the AAS LaTeX macros v5.0.

Fig. 3.— WHAM spectra of Comet Hale-Bopp, February 22–March 5, 1997. Solid line is a model with 3 Voigt profiles in emission plus 7 Voigts in absorption representing the scattered solar spectrum. The dotted line is the same minus the cometary [O I] emission line.

Fig. 4.— Water production rate history assuming Van Dishoeck & Dalgarno (1984) OH photodissociation cross-sections.

Fig. 5.— Water production rate history assuming Nee and Lee (1984) OH photodissociation cross-sections.

Fig. 6.— Haser (1957) models. H_2O outflow velocity is 1 km s^{-1} , OH outflow velocity is 3 km s^{-1} using the Van Dishoeck & Dalgarno (1984) OH lifetime, 8 km s^{-1} using the Nee & Lee (1984) OH lifetime.